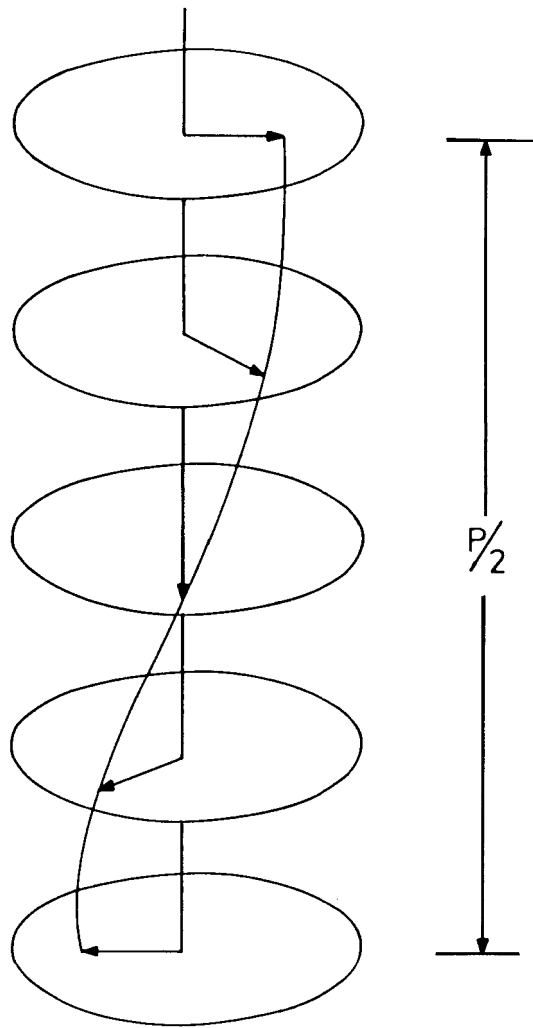


## CHAPTER II

# ELECTROMECHANICAL EFFECT IN CHOLESTERIC LIQUID CRYSTALS WITH FREE BOUNDARY CONDITIONS

### 2.1 Introduction

As we discussed in chapter I, cholesteric liquid crystals are formed by optically active molecules. In this phase, chiral interactions between the molecules are minimised when there is a finite angle between their long axes. This results in a helical arrangement of the director  $\hat{n}$  with the screw axis normal to  $\hat{n}$  (Fig.2.1). In principle, the director can twist about two mutually orthogonal directions normal to  $\hat{n}$ . But such double twist cylinders would then have to arrange in a regular lattice to produce a thermodynamic phase. Such a lattice is always associated with disclinations which cost curvature elastic energy. Hence at low temperatures, the medium twists only about one axis giving rise to the cholesteric phase. Close to the temperature of transition to the isotropic phase, the elastic energy is considerably reduced and compounds with a short pitch of the helix exhibit the double twisted blue phases. Our investigations are confined only to the lower temperature cholesteric phase.



**Figure 2.1.** Schematic representation of the helical arrangement of the director in cholesteric liquid crystalline phase.

The pitch ' $P$ ' of the helix is of the order of a micron. It depends on the nature of the molecules, the temperature and external forces.

The cholesteric material is similar to the nematic in its thermodynamic properties. In fact, a nematic liquid crystal can be called a cholesteric with an infinite pitch. However, the lack of mirror symmetry in cholesteric liquid crystals leads to some unusual physical effects. According to Curie's Principle (see for e.g., Boccara 1981) the macroscopic chirality of the medium gives rise to some interesting cross-coupling terms between hydrodynamic fluxes and forces. One of the first physical experiments on liquid crystals (Lehmann 1900) demonstrated such a cross-coupling effect. As we mentioned in chapter I, in 1900 Lehmann observed the phenomenon of rotation of cholesteric drops when they were subjected to a vertical thermal gradient, parallel to their helical axes (Fig.1.14). Oseen considered that the motion was due to the molecules rotating with uniform angular speed around vertical axes drawn through their centres of gravity.

The hydrodynamic theory of cholesterics was developed by Leslie (1968, 1979) who got solutions corresponding to the Lehmann rotation phenomenon. Similar solutions were obtained by Lubensky (1972, 1973) and Martin *et al.* (1972) in their developments of the hydrodynamic theory of cholesterics. The latter theories emphasized the effective one dimensional layering order with spacing  $= P/2$  of the cholesteric phase, more than the helical arrangement of the nematic director.

de Gennes (1975) later pointed out that any transport current like an electric current, a heat current or a diffusion current should in principle give rise to a similar effect. We shall briefly describe the hydrodynamics of cholesterics as developed by Leslie (1968).

## 2.2 Theoretical background

In the following we use the notation given by de Gennes (1975). Let us consider a transport current with which is associated a conjugate field  $\vec{E}$ . For the three cases of electric current, heat current or a diffusion current, we can write

$$\begin{aligned}\vec{E} &= -\nabla V \text{ (where } V \text{ is the electrical potential),} \\ \vec{E} &= -\nabla T/T \text{ (where } T \text{ is the temperature) and} \\ \vec{E} &= -\nabla \mu \text{ (where } \mu \text{ is the chemical potential of the diffusing species)} \\ &\text{respectively.}\end{aligned}$$

The entropy source including flow, rotation of the director and the transport takes the form

$$T\dot{S} = A : \sigma' + \vec{h} \cdot \vec{N} + \vec{J} \cdot \vec{E} \quad (2.1)$$

where  $\dot{S}$  is the rate of change of the entropy density,  $A$  is the symmetric part of the velocity gradient tensor, i.e.,

$$A_{ij} \equiv \frac{1}{2} \left( \frac{\partial v_i}{\partial x_j} + \frac{\partial v_j}{\partial x_i} \right), \quad (2.2)$$

where  $\sigma'$  is the viscous stress tensor,  $\vec{h}$  now represents the hydrodynamic part of the molecular field,  $\vec{N}$  the rate of change of director with reference to the background fluid, i.e.,

$$\vec{N} = \frac{\partial \hat{n}}{\partial t} - (\vec{\omega} \times \hat{n}) \quad (2.3)$$

where  $\mathcal{B}$  is the antisymmetric part of the velocity gradient tensor,  $\vec{J}$  the current density and  $\vec{E}$  is the field conjugate to the current as defined earlier.  $A$ ,  $\vec{N}$  and  $\vec{E}$  are taken to be the fluxes and  $\sigma'$ ,  $\vec{h}$  and  $\vec{J}$  are then the conjugate forces.

The phenomenological equations between fluxes and forces is then written in the following form

$$\sigma'_{\alpha\beta} = \sigma_{\alpha\beta}^N + \mu_1 n_\alpha (\vec{E} \times \hat{n})_\beta + \mu_2 n_\beta (\vec{E} \times \hat{n})_\alpha \quad (2.4)$$

$$\vec{h} = \vec{h}^N + \nu \hat{n} \times \vec{E} \quad (2.5)$$

$$\vec{J} = \sigma_{\perp} \vec{E} + (\sigma_{\parallel} - \sigma_{\perp})(\hat{n} \cdot \vec{E})\hat{n} + \nu \hat{n} \times \vec{N} - (\mu_1 + \mu_2)\hat{n} \times (\mathbf{A} : \hat{n}) \quad (2.6)$$

Here  $\sigma_{\alpha\beta}^N$  and  $h^N$  are the *nematic* contributions from the non-chiral part (see de Gennes, 1975) and  $\sigma_{\perp}$  and  $\sigma_{\parallel}$  are the relevant conductivities. There are three new coefficients,  $\mu_1, \mu_2$  and  $\nu$  connected by the equation

$$\mu_1 - \mu_2 = \nu . \quad (2.7)$$

When the coordinate system is reflected in a mirror, all the terms in eqns (2.4) to (2.6) which are associated with the new coupling coefficients  $\mu_1, \mu_2$  and  $\nu$  will change sign. This means that there should be a change in the sign of the cross-coupling coefficients themselves in the reflected system. In other words, these coefficients can have finite values only for chiral systems. In the hydrodynamic limit, the relevant chirality is the macroscopic chirality, viz., the wavevector  $q$  of the helix which also changes sign on reflection. In the lowest approximation, the cross-coupling coefficients must be proportional to  $q$  (de Gennes 1975). As a convention, the sign of the helix is taken to be positive for a right handed helix and negative for a left handed helix. Then according to the hydrodynamic theory, the cross-coupling does not exist for a system with  $q = 0$  such as in the case of a nematic or a compensated cholesteric. The cross-coupling involving the thermal gradient results in the rotation phenomenon observed by Lehmann. In the following, we discuss the effect of an ionic current which should give rise to a similar rotation phenomenon.

We consider a homogeneously aligned cholesteric material. Let an electric field be applied parallel to the helical axis. Let us assume that there is no hydrodynamic flow, i.e.,  $\mathbf{A} = 0$ . The azimuthal angle  $\phi(z)$  between the director and a fixed axis  $x$

can be obtained from the torque balance equation. The viscous torque is given by

$$\Gamma_z^{viscous} = \sigma'_{yx} - \sigma'_{xy} \quad (2.8)$$

Substituting for  $\sigma'$  from (2.4) when  $A = 0$ , we have

$$\begin{aligned} \Gamma_z^{viscous} &= \alpha_2 n_y \dot{n}_x + \alpha_3 n_x \dot{n}_y - \alpha_2 n_x \dot{n}_y - \alpha_3 n_y \dot{n}_x + \mu_1 n_y (-n_y E_z) \\ &+ \mu_2 n_x (n_x E_z) - \mu_1 n_x (n_x E_z) - \mu_2 n_y (-n_y E_z) \\ &= (\alpha_2 - \alpha_3)(n_y \dot{n}_x - n_x \dot{n}_y) - \nu n_y^2 E_z - \nu n_x^2 E_z \end{aligned} \quad (2.9)$$

as  $\mu_1 - \mu_2 = \nu$ .

Now  $n_x = \cos\phi$  and  $n_y = \sin\phi$ . Hence

$$\Gamma_z^{viscous} = (\alpha_2 - \alpha_3) \left( -\frac{d\phi}{dt} \right) - \nu E_z = \gamma_1 \frac{d\phi}{dt} - \nu E_z \quad (2.10)$$

where  $\alpha_3 - \alpha_2 = \gamma_1$ .

The elastic torque is given by

$$\Gamma_z^{el} = n_x h_y^{el} - n_y h_x^{el} \quad (2.11)$$

$h_x^{el}$  and  $h_y^{el}$  can be obtained from the expression for the free energy density

$$F_d = \frac{K_{22}}{2} [\hat{n} \cdot \text{curl} \hat{n} + q_o]^2 = \frac{K_{22}}{2} \left[ n_y \frac{\partial n_x}{\partial z} - n_x \frac{\partial n_y}{\partial z} + q_o \right]^2$$

We then have

$$\begin{aligned} h_x^{el} &= -\frac{\partial F_d}{\partial n_x} + \frac{\partial}{\partial z} \left[ \frac{\partial F_d}{\partial \left( \frac{\partial n_x}{\partial z} \right)} \right] \quad \text{and} \\ h_y^{el} &= -\frac{\partial F_d}{\partial n_y} + \frac{\partial}{\partial z} \left[ \frac{\partial F_d}{\partial \left( \frac{\partial n_y}{\partial z} \right)} \right] \end{aligned} \quad (2.12)$$

Hence

$$\Gamma_z^{elastic} = -K_{22} \left[ n_y \frac{\partial^2 n_x}{\partial z^2} - n_x \frac{\partial^2 n_y}{\partial z^2} \right] \quad (2.13)$$

which yields

$$\Gamma_z^{elastic} = K_{22} \left( \frac{\partial^2 \phi}{\partial z^2} \right) \quad (2.14)$$

Equating the elastic and viscous torques,

$$\gamma_1 \frac{d\phi}{dt} - \nu E_z = K_{22} \left( \frac{\partial^2 \phi}{\partial z^2} \right) \quad \text{or}$$

$$\gamma_1 \frac{d\phi}{dt} = K_{22} \left( \frac{\partial^2 \phi}{\partial z^2} \right) + \nu_E E_{\perp} \quad (2.15)$$

where  $E_{\perp}$  is the component of  $\vec{E}$  normal to  $\hat{n}$ , i.e.,  $E_z$  and  $\nu_E$  is the electromechanical coupling coefficient in the present problem. Equation (2.15) can be integrated using proper boundary conditions. If the anchoring energy for azimuthal orientation is zero  $\frac{\partial \phi}{\partial z} - q_0 = \frac{2\pi}{P}$  at both the boundaries and hence a constant in the sample. The solution is then of the form

$$\phi = q_0 z + \frac{\nu_E E t}{\gamma_1} + c \quad (2.16)$$

where  $c$  is a constant of integration. The director rotates with a constant angular velocity given by  $\frac{\nu_E E}{\gamma_1}$ . The angular velocity should be proportional to the electric field  $E$  and the sense of rotation should change when  $\vec{E}$  is reversed. The handedness of the helix should also determine the sense of rotation, as the coupling coefficient is assumed to be proportional to  $q$ .

The anchoring energy for azimuthal orientation can be expected to have a finite value when the liquid crystal is oriented on a solid surface. This can prevent the thermomechanical or electromechanical rotation of the director. It is worthwhile to estimate the upper limit of anchoring energy which allows the rotation of the director.

In order to make an estimate of the allowed upper limit of the anchoring energy for the thermomechanical case, Madhusudana and Pratibha (1989) assumed that the upper surface at  $z = d$  is free with zero anchoring energy in order to simplify the argument. The lower surface resting on the glass plate at  $z = 0$  is assumed to have weak anchoring with the corresponding energy given by  $\frac{1}{2}W \sin^2 \phi_o$ ,  $\phi_o$  being the angle made by the director with the easy axis. Then the restoring torque at the lower surface due to this anchoring energy is given by  $W \sin \phi_o \cos \phi_o$ . This torque being maximum at  $\phi_o = \pi/4$ , it can be assumed that the surface anchoring can be overcome if the angle  $\phi_o$  produced by the action of the thermomechanical coupling is greater than  $\pi/4$ . In such a case a rotation becomes possible although it is not completely free. Under the static limit, the surface torque balance equation is given by

$$W \sin \phi_o \cos \phi_o = K_{22} \left[ \left( \frac{\partial \phi}{\partial z} \right) - q_o \right] \quad (2.17)$$

and the bulk torque balance equation is given by

$$K_{22} \left( \frac{\partial^2 \phi}{\partial z^2} \right) = \nu E \quad (2.18)$$

We have a free surface at  $z = d$  and hence  $\left[ \frac{\partial \phi}{\partial z} \right]_{z=d} = q_o$

The solution is then

$$\phi = \left( \frac{\nu E}{2K_{22}} \right) z^2 + qz + \phi_o \quad (2.19)$$

where

$$q = \left[ q_o - \left( \frac{\nu E}{K_{22}} \right) d \right].$$

Therefore at  $z = 0$ , we get

$$W = - \frac{\nu E d}{\sin \phi_o \cos \phi_o}. \quad (2.20)$$



The order of magnitude of thermomechanical coupling coefficient  $\nu$  can be estimated by a dimensional argument.  $\nu$  has the dimension of an energy per unit area. Moreover according to the hydrodynamic theory,  $\nu$  must vanish when  $q_o$  vanishes and must be odd in  $q_o$ . Thus to a first approximation (de Gennes, 1975)

$$\nu_E = xK_{22}q_o \quad (2.21)$$

where  $x$  can be assumed to be  $\approx 1$ . This gives  $\nu_E \approx 0.33 \times 10^{-8} NV^{-1} m^{-1}$  If  $\phi_o = \pi/4$ , we get  $W = 10^{-7} Jm^{-2}$ . This is equal to an extrapolation length  $L = K_{22}/W \simeq 10 \mu m$ . The anchoring energy must be lower than this for the rotation phenomenon to occur.

In practice, it is very difficult to achieve homogenous alignment with such a weak anchoring on solid surfaces. As we mentioned earlier, there is no published report of reproducing the Lehmann rotation experiment demonstrating the thermomechanical effect.

There are several theoretical papers (Frost , 1972; Ranganath, 1983; Jayaram *et al.*, 1983) suggesting some possible experimental techniques which do not require weak anchoring at the surfaces for studying the thermomechanical effect. However, no experimental studies have been made based on these suggestions. Eber and Janossy (1982, 1984) tried to measure the thermomechanical coupling coefficient using a compensated cholesteric mixture. In their analysis they make an assumption which in effect means that the thermomechanical coefficient is molecular rather than structural in origin so that even in a compensated mixture with the wavevector  $q = 0$ , one can get a non-zero coupling constant. Pleiner and Brand (1987) have questioned the analysis of the experiment by Eber and Janossy. They argue that their experimental result may be consistent with the thermomechanical coupling being zero for the compensated cholesteric mixture. In other words, Pleiner and

Brand also argue that the origin of this coupling is mainly due to the macroscopic helical structure rather than molecular chirality.

### **2.3 Earlier experiments on electromechanical coupling**

Madhusudana and Pratibha (1987, 1989) reported the first observations of a rotation phenomenon caused by the electromechanical effect, which arises due to the transport of ions in a cholesteric sample. They found the electromechanical rotation in flat cholesteric drops which were floating in an isotropic medium, when they were subjected to a DC electric field.

As the azimuthal anchoring energy at the cholesteric-isotropic interface can be expected to be zero, Madhusudana and Pratibha (1987) tried several techniques to float cholesteric drops with the appropriate structure in an isotropic medium. They found that cholesteric drops floating in liquids like glycerine, ethyleneglycol, etc., were spherical in shape because of the large interfacial tension. These do not have a suitable geometry for the experiment. They adopted the following technique to get the appropriate type of drops.

Lixon, a non-mesomorphic epoxy compound was found to dissolve in a specially prepared cholesteric mixture. This results in a lowering of the cholesteric-isotropic transition temperature and a broad two phase coexistence region. Lixon has a strong affinity for glass and the isotropic phase has got a higher concentration of Lixon than the cholesteric phase. Therefore adjacent to the glass plates, one would expect to find only the isotropic phase. The interfacial tension between the cholesteric liquid crystal and the isotropic phase which are chemically essentially similar is very small ( $< 10^{-5} \text{ n/m}$ ). So the energy required to change the shape of the spherical drop is negligible. Further, the relative difference in density between the cholesteric and

the isotropic phase is also very small ( $\sim 10^{-3}$ ). As a consequence of the above properties, the cholesteric drops are surrounded by the isotropic phase on all sides. Hence we get a configuration shown in figure 2.2.

Spherical cholesteric drops with a characteristic radial  $\chi$  line of strength +2 are formed in cells with large thicknesses (Fig.2.3a). Such cholesteric drops were first experimentally studied by Robinson (1956). Pryce and Frank gave the following description of the director pattern in cholesteric drops, as quoted by Robinson *et al.* (1958). Considering a spherical surface of the drop, the director orientation can be described by a family of circles passing through a singular point **P** (Fig.2.4). These are tangential to a line **PQ** passing through **P**. As the molecules are chiral, the director orientation changes as the diameter of the spherical shell is varied. This means that the tangential line (**PQ**) rotates as the size of the spherical shell is changed and a radial line defect results from this structure. The drops get flattened for smaller thicknesses of the cell. The  $\chi$  line is then confined only to the lateral curved region of the drop. Flat cholesteric drops with a lateral diameter of 20-50  $\mu\text{m}$  can be formed in cells of thickness  $d \approx 8\mu\text{m}$  with the isotropic phase surrounding the drops on all sides. As the director has a tangential alignment at this interface, the central flat region of the drop is homogeneously aligned with the helical axis perpendicular to the flat surface. However, in each horizontal layer, the director has a splay-bend distortion arising from the presence of the  $\chi$  line at the edge. Four out of the eight dark brushes emerging out of the  $\chi$  line become visible for proper orientations of the polarizer and analyser (Fig.2.3b-h).

By applying an appropriate DC electric field to such flat cholesteric drops, Madhusudana and Pratibha observed a rotation of the structure in the drops. When the field direction was changed the direction of rotation of the drops also changed. These

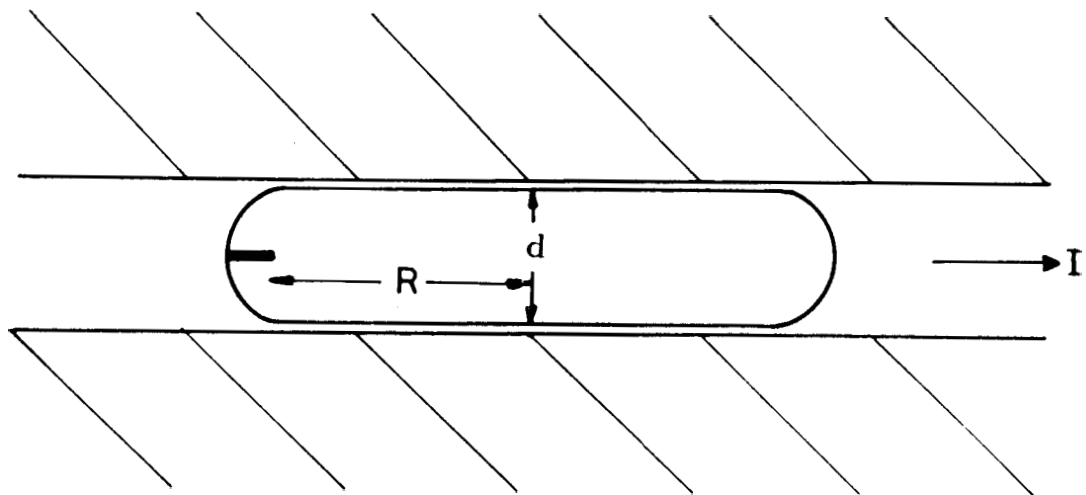


**Figure 2.2.** Vertical cross-section of a flattened cholesteric droplet between two glass plates. It is surrounded on all sides by the isotropic phase.

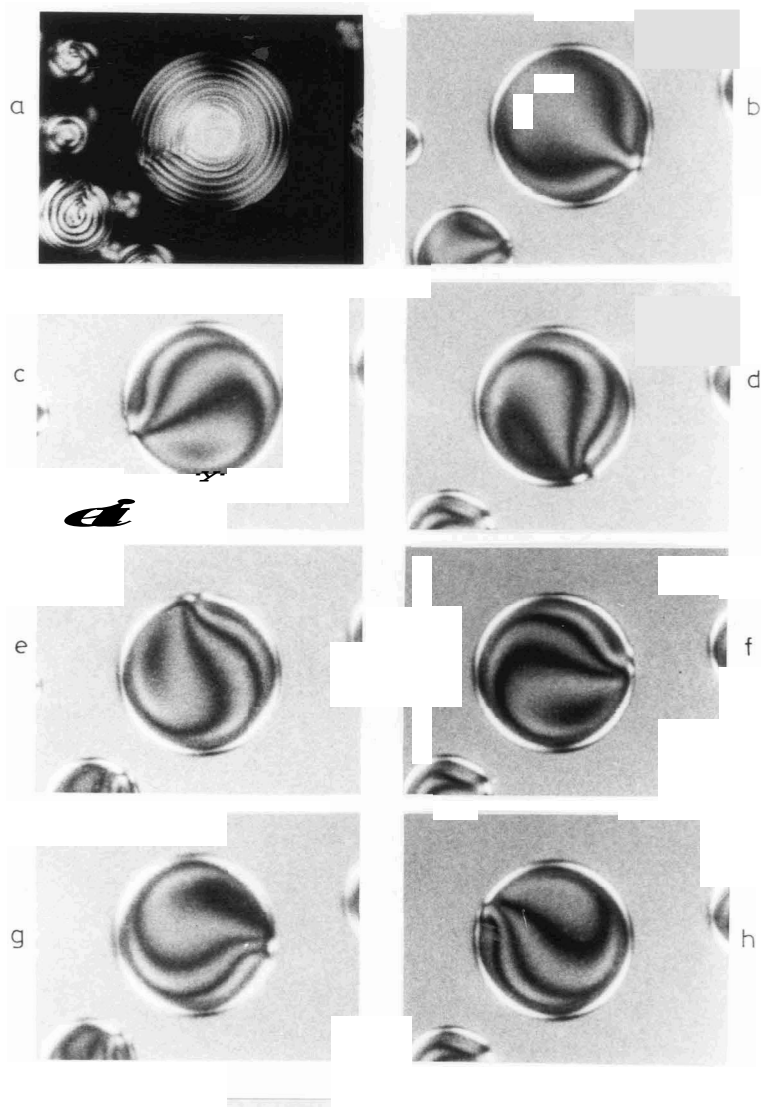


**Figure 2.3.** (a) A cholesteric droplet showing the  $\chi$  line defect in a nearly spherical drop. (b) A flat droplet of a left-handed cholesteric in the absence of the field. The dark brushes emanate from the short  $\psi$ -line near the edge of the droplet. (c-h) Photograph of the drop shown in (b) at different times after the application of a voltage to the cell. (c),(e),(g) correspond to +2V and (d), (f) and (h) to -2V. (From Madhusudana and Pratibha, 1989).

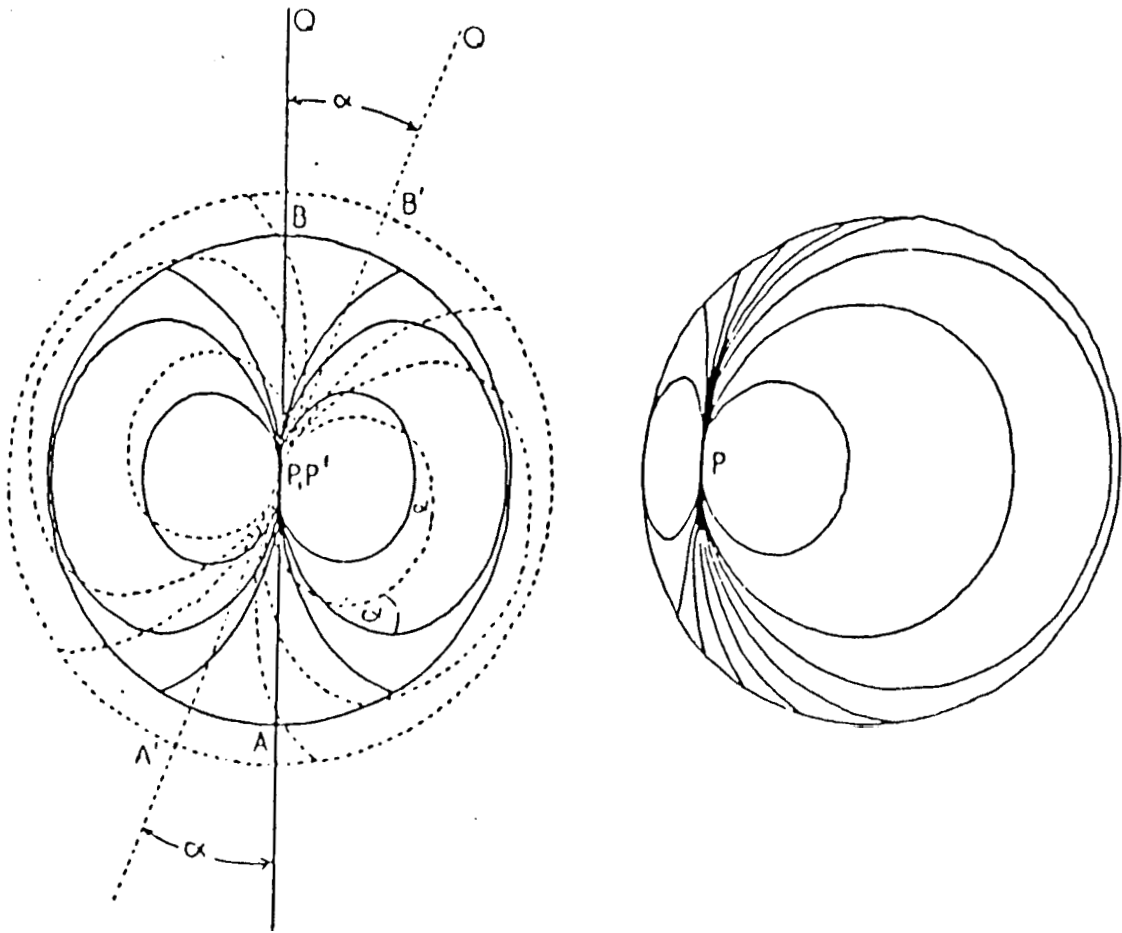


**Figure 2.4.** Family of circles constructed in accordance with Pryce and Frank's model. (From Robinson et *al.*, 1958).

rotating structures (see Fig.2.3) resembled the sketches made by Lehmann way back in 1900. The electromechanical effect is analogous to the thermomechanical effect observed by Lehmann. The rotation of the structures can be used to measure  $\nu_E$ , the electromechanical coupling coefficient.

When the sample has an ideal planar structure, the solution corresponding to the Lehmann rotation is, from equation (2.16)

$$\frac{d\phi}{dt} = \frac{\nu_E E}{\gamma_1} \quad (2.22)$$

where  $\nu_E$  is the electromechanical coefficient,  $E$  the applied electric field,  $\gamma_1$  the rotational viscosity coefficient and  $\phi$  the azimuthal angle of  $\hat{n}$ . This equation has to be slightly modified to account for the rotation of the  $\chi$  line defect associated with the actual drops. Near the  $\chi$  line the deformation of the director field is very large. The reorientation implied by the motion of the defect needs a considerable amount of energy. But the electromechanical coupling which is responsible for the rotation of the director is effective only in the planar oriented flat part of the drop. The effective friction coefficient  $\zeta$  (per unit length) for a slow motion of a nematic line singularity with a core has been estimated by Imura and Okano (1973) and de Gennes (1976). They showed that  $\zeta \propto S^2$  where  $S$  is the strength of the defect line. There is every possibility that the  $\chi$ -line of strength  $+2$  is coreless because of the collapse of the director in the third dimension (de Gennes, 1975). The scheme of Imura and Okano can be extended to this case and the result is (Madhusudaria and Pratibha, 1989)

$$\zeta = 2\gamma_1 |S| \quad (2.23)$$

which is a linear function of  $|S|$ .

The entropy generation arises due to the rotational motion of the director and the linear motion of the defect around the periphery of the drop. An approximate

energy rate balance for the drop can be written as

$$2\pi\gamma_1 |S| u^2 \frac{d}{2} + \pi r^2 d\gamma_1 \left(\frac{d\phi}{dt}\right)^2 \simeq \pi r^2 d\nu_E E \frac{d\phi}{dt} \quad (2.24)$$

where the defect length has been taken as  $d/2$ ,  $r$  is the radius of the flat drop,  $u = r(d\phi/dt)$  is the velocity of the defect.

Therefore

$$\gamma_1 |S| \frac{d\phi}{dt} + r_1 \frac{d\phi}{dt} = \nu_E E \quad (2.25)$$

Thus in the presence of a line defect rotating with the structure, we get with  $S=2$

$$\frac{d\phi}{dt} = \frac{\nu_E E}{3\gamma_1}. \quad (2.26)$$

Using the slope of  $\frac{d\phi}{dt}$  vs.  $E$  curve (Fig.2.5) in a specific sample used by them Madhusudana and Pratibha found that  $|\nu_E| \approx 0.09 \times 10^{-5} N/Vm$ . Detailed observations lead them to come to the following conclusion.

1. The direction of rotation of the drops is the same for a given sign of the field. When viewed along the field direction, the right handed helix rotates in anticlockwise direction. Further, when the voltage is reversed, both the curvatures of the dark brushes as well as the sense of rotation of the structure are reversed.
2. From figure 2.5 it is found that the DC field is totally screened up to  $\simeq 1.9V$  which should be the redox potential of one of the components in the mixture. It is found that up to an applied voltage of  $\approx 3.5V$ , the angular velocity increases linearly. However, beyond such a voltage, there is a change in the structure of the drop and the rotational velocity becomes a non-linear function of the applied voltage.



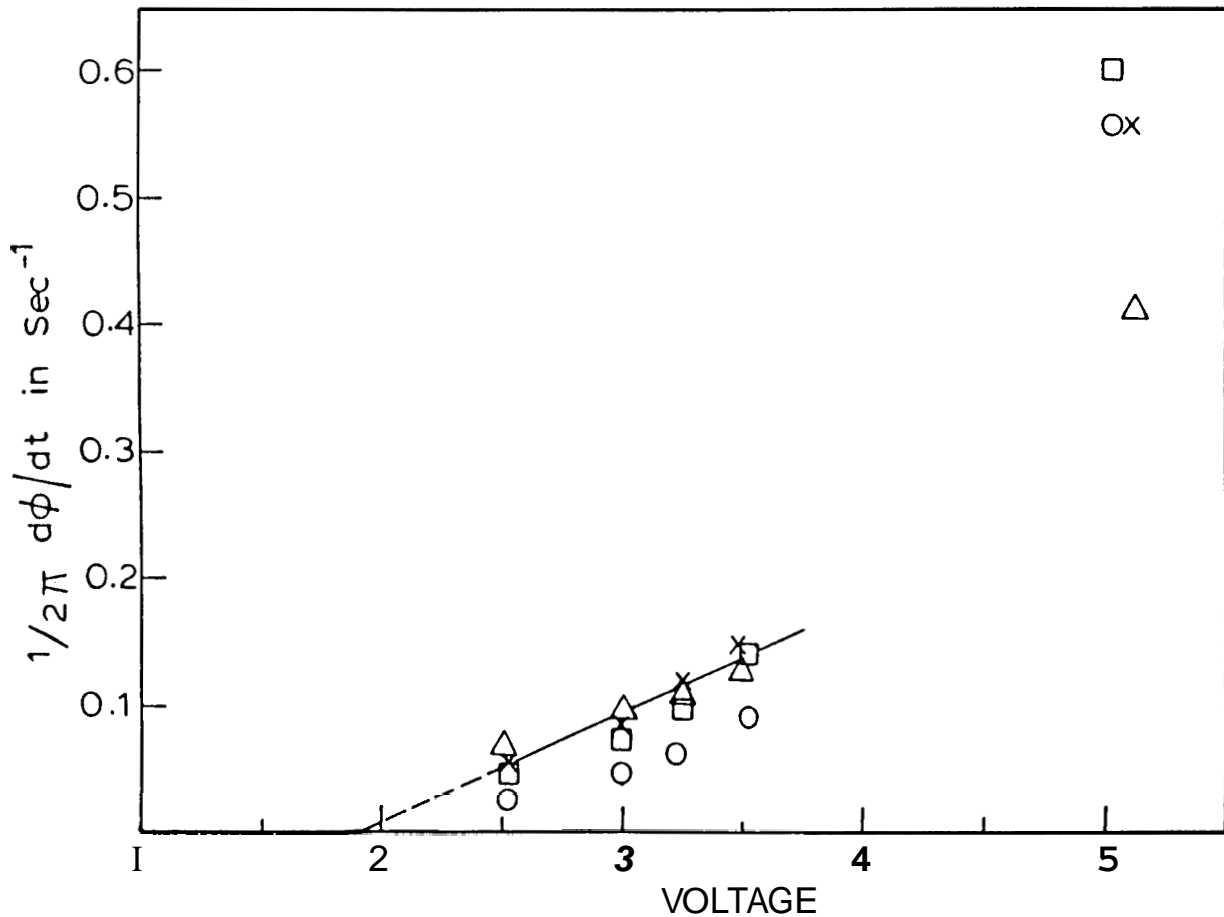
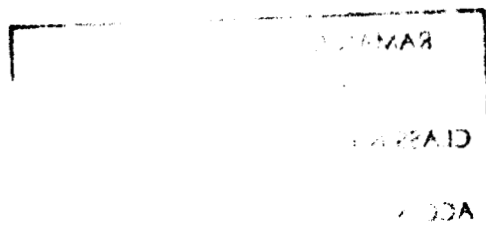


**Figure 2.5.** Plot of the rotational velocity of the structure as a function of applied voltage. Different symbols correspond to different drops. The slope of the straight-line which corresponds to the drops with the fastest angular velocity was used in the calculation of  $\nu_E$ . (From Madhusudana and Pratibha, 1989).



3. The rotation phenomenon is found to be absent in nematic droplets under the action of  $E$ .
4. For a given sense of the field, the angular velocity reverses sign with the handedness of the helix.
5. The angular velocity of a drop does not depend upon its radius which implies that it is the structure that rotates in a droplet rather than its rigid body, in agreement with the earlier observation of Lehmann.

Thus, Madhusudana and Pratibha devised a technique to reproduce the Lehmann rotation experiment under a DC electric field and verified that the phenomenon satisfies all the required symmetry properties, viz., the rotational velocity linearly depends on  $\vec{E}$  and the coupling coefficient  $\nu_E$  changes sign with that of  $q$ . But they did not make a detailed study of the variation of the electromechanical coupling  $\nu_E$  with that of the wavevector  $q$ . As already mentioned, Eber and Janossy have argued that the thermomechanical coefficient is molecular in origin. The author has made measurement of  $\nu_E$  as a function of  $q$  in an appropriate system with the hope of clarifying the origin of the electromechanical coefficient. The present chapter summarises these results.

## **2.4 Experimental Technique**

### **2.4.1 Materials**

We make use of mixtures consisting of 4 or 5 components in our experiment. For having a homogeneous composition of the mixture, it is to be heated, stirred well mechanically and maintained in the isotropic phase for at least 20-25 mins. For this purpose, a suitable oven consisting of an aluminium block with appropriate holes

was constructed.

The dielectric anisotropy of the liquid crystal  $\Delta\epsilon = \epsilon_{\parallel} - \epsilon_{\perp}$ , where  $\epsilon_{\parallel}$  and  $\epsilon_{\perp}$  are the dielectric constants along and perpendicular to the director.  $\Delta\epsilon$  may be positive or negative depending on whether the permanent dipole moments are parallel or perpendicular to the long axes of the molecules. The director couples to an external electric field through the dielectric anisotropy. In the present experiment, since the field has to be applied along the helical axis, it is convenient to choose a material with negative dielectric anisotropy to avoid change in the orientation of the director due to this coupling. We made a binary mixture of ethoxyphenyl-*trans*-butylcyclohexyl carboxylate (EPBC) and methoxyphenyl-*trans*-pentyl cyclohexyl carboxylate (MPPC) in the ratio of 18:82 mole per cent. The structural formulae of the components used is shown in figure 2.6. Taking the values of dielectric anisotropies of the individual components at room temperature from the Merck catalogue and using the additivity law, we have estimated the dielectric anisotropy of the mixture to be  $\simeq -1$ . We chiralised this nematic mixture by doping different amounts of cholesteryl chloride to get cholesteric mixtures with different values of pitch in order to study the variation of the electromechanical coupling coefficient with the wavevector. We have also added two cholesteric materials with opposite handedness to the nematic mixture to get a cholesteric with infinite pitch.

#### **2.4.2 Measurement of pitch**

We require a wedge shaped cell to find the pitch of the cholesteric sample. These wedges were prepared using glass plates treated to get a homogeneous alignment of the liquid crystal. The glass surfaces should be absolutely clean to get a good alignment. Even the presence of a slight amount of grease favours homeotropic

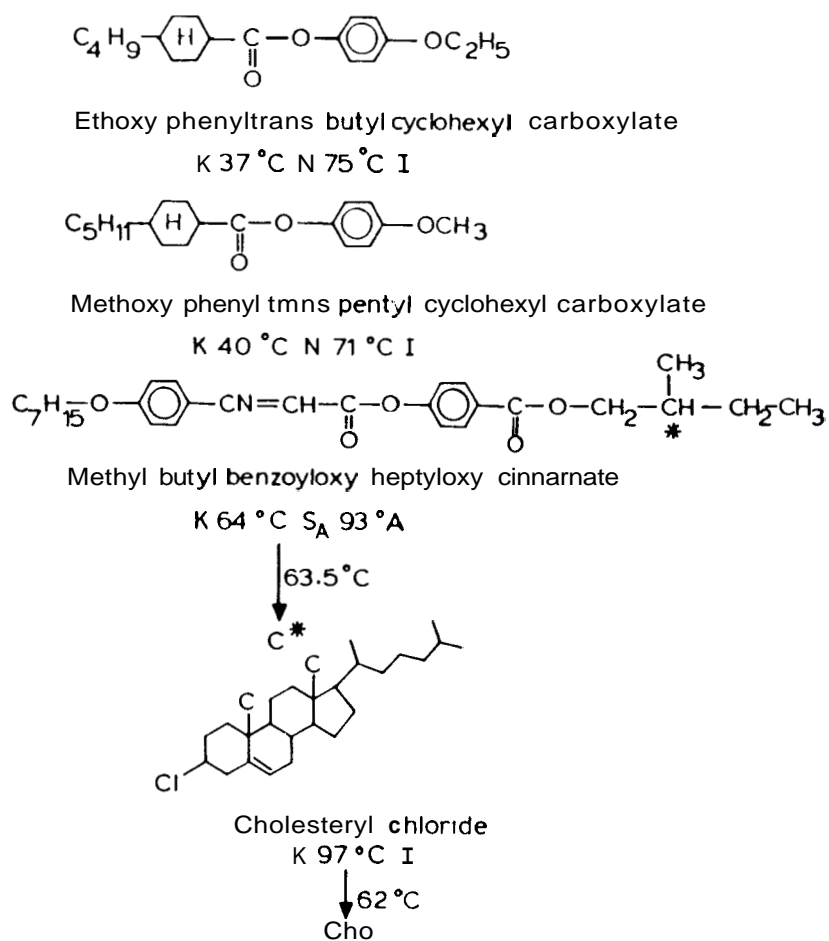


**Figure 2.6.** Structural formulae and transition temperatures of (1) EPBC, (2) MPPC, (3) C<sub>7</sub>, (4) CC.

alignment. To remove any traces of grease, the glass plates were washed successively in strong chromic acid, water, teepol, again in water and then in alcohol and lastly in chloroform. The quality of the surface was tested by making sure that a film of water uniformly sticks to the glass surface. The glass surfaces are then coated with a 3% polyimide solution. To remove the solvent and for soft baking, the plates are kept at  $65^{\circ}\text{C}$  for 15 minutes. Further, they are cured for 60 min. at  $300^{\circ}\text{C}$  to get a hard coating. After curing, the polyimide layer can be buffed unidirectionally to get the required alignment.

A wedge is formed between the two plates (Fig.2.7a) by fixing a mylar spacer (of  $\simeq 250\mu\text{m}$  thickness) at one of the ends using an epoxy as adhesive. The angle  $\alpha$  of the wedge is measured using a goniometer (Freiberger).

The wedge-shaped cell is partially filled with the liquid crystal mixture maintained in the isotropic phase. The sample enters the wedge by capillary action.

The pitch of the cholesteric sample is measured using the Cano-Grandjean (Grandjean, 1921; Cano 1961; Kassubek and Meyer, 1969) technique. When there is a strong anchoring of the molecules at the two glass surfaces, then without changing the equilibrium value of the pitch  $P$ , the cholesteric helix can be inserted in the gap only when its thickness satisfies the condition  $d = nP/2$ , where  $n = 1, 2, \dots$  is the number of half-pitches of the helix. When the thickness of the cell deviates from these values by a small amount (Fig.2.7b), the helix fits into the wedge with the same number of half-turns but with some alteration in the effective value of the pitch. On the thinner side the pitch is reduced and on the thicker side it is increased. But approximately in between, i.e., for thickness  $\simeq (n + \frac{1}{2})\frac{P}{2}$ , the number of half-turns fitting into the wedge changes by one. A Cano-Grandjean disclination appears here. It looks like a fine scratch parallel to the ridge of the wedge in polarised light

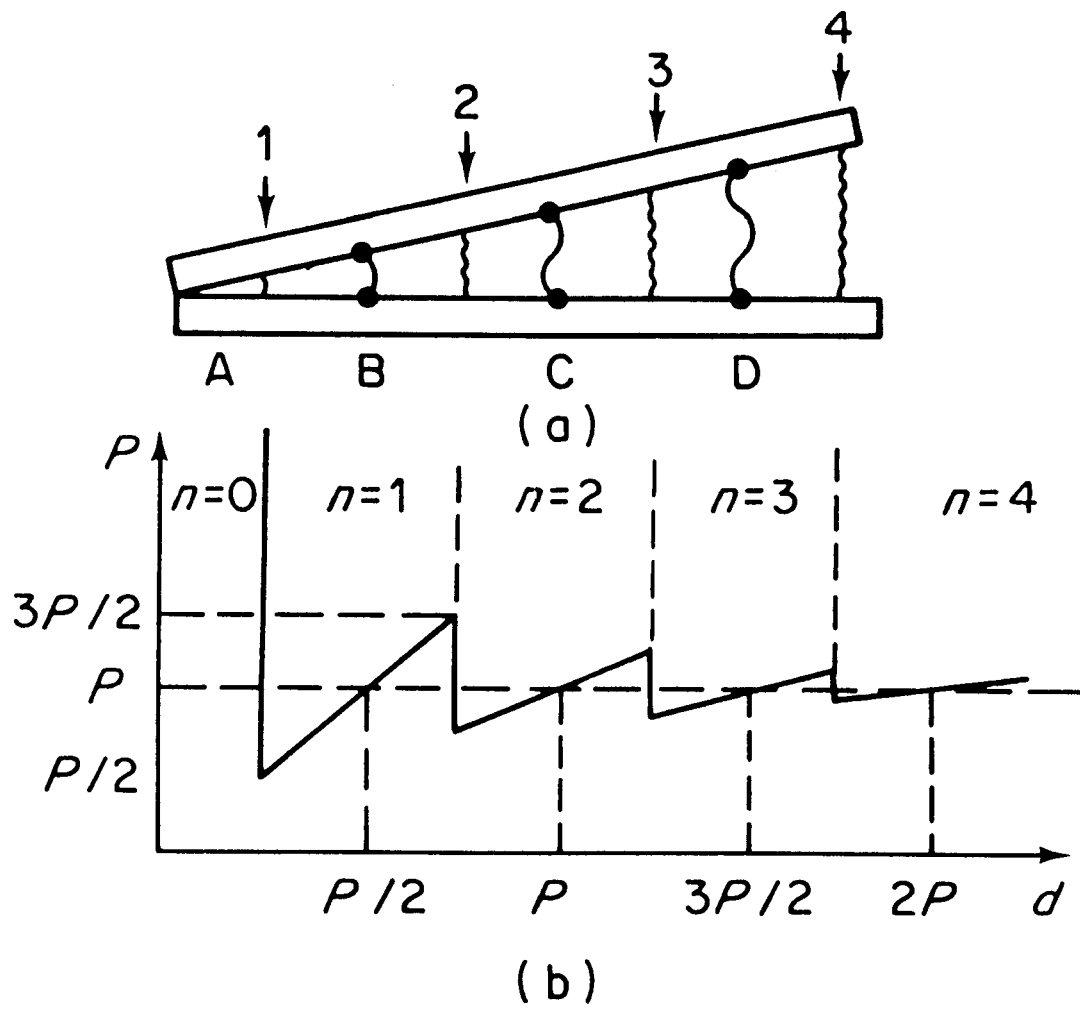


**Figure 2.7.** (a) Wedge shaped cell. The numbers indicate Cano-Grandjean disclinations and the letters indicate the Grandjean zones. (b) Calculated dependence of the forced pitch upon the thickness of the cell.  $n$  is the number of half-turns of the helix in a Grandjean zone. (From Blinov, 1983).

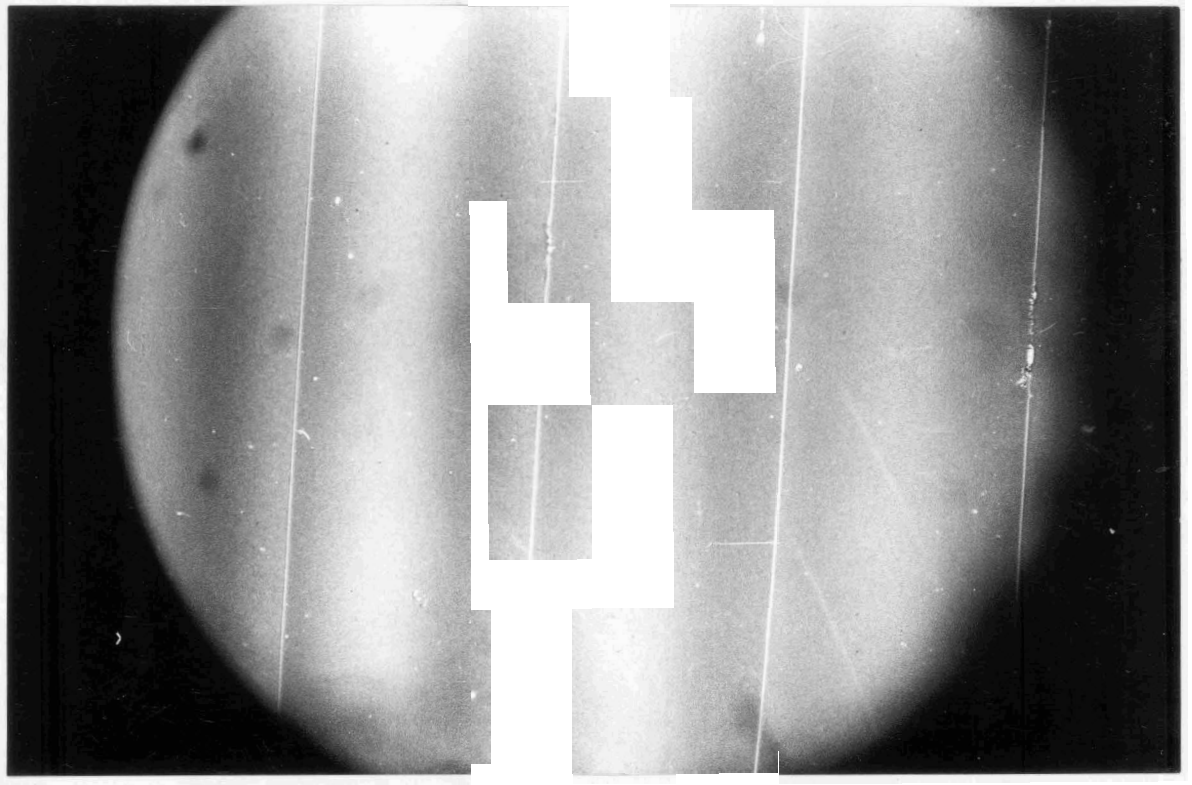


Figure 2.8. Photograph of Cano-Grandjean disclinations in one of the samples prepared by us.

(Fig.2.8). If  $\alpha$  is the angle of the wedge as measured using the goniometer and  $l$  is the separation between the disclination lines, the pitch is given by  $P = 2l\alpha$ .

In figure 2.9 the pitch is plotted vs. concentration of the cholesteric component, viz., cholesteryl chloride in the binary nematic mixture at room temperature.

### 2.4.3 Determination of the handedness of the sample

A glass slide and a plano-convex lens were thoroughly cleaned. The convex surface of the lens and the slide were coated with polyimide and rubbed to give a homogeneous alignment. This system was placed on a microscope carriage which can be moved along both  $x$  and  $y$  directions. The glass surfaces are oriented so that the rubbing directions on the two surfaces were parallel to each other. Concentric disclination rings were seen (Fig. 2.10). The diameter of these rings formed were measured on the  $y$ -scale.

Then the lens was rotated with respect to the glass plate in either direction and then again the diameters of the disclination rings were measured. If the direction in which the lens is rotated is the same as that of the natural twist, the thickness at which the natural helical arrangement matches with the surface orientation increases compared to the previous case. Correspondingly the diameters of the disclination rings also expand. The rings appear to move outward. If the direction in which the lens is rotated is opposite to that of the natural twist, the diameters of the disclination rings become smaller. The sense of the helix is found by the relative change in diameter.

For example, in the present case, the addition of 2.58 weight % of cholesteryl chloride to 18:82 mole % of EPBC and MPPC exhibited a left handed chirality and the value of the pitch was found to be  $10.4 \mu\text{m}$ .



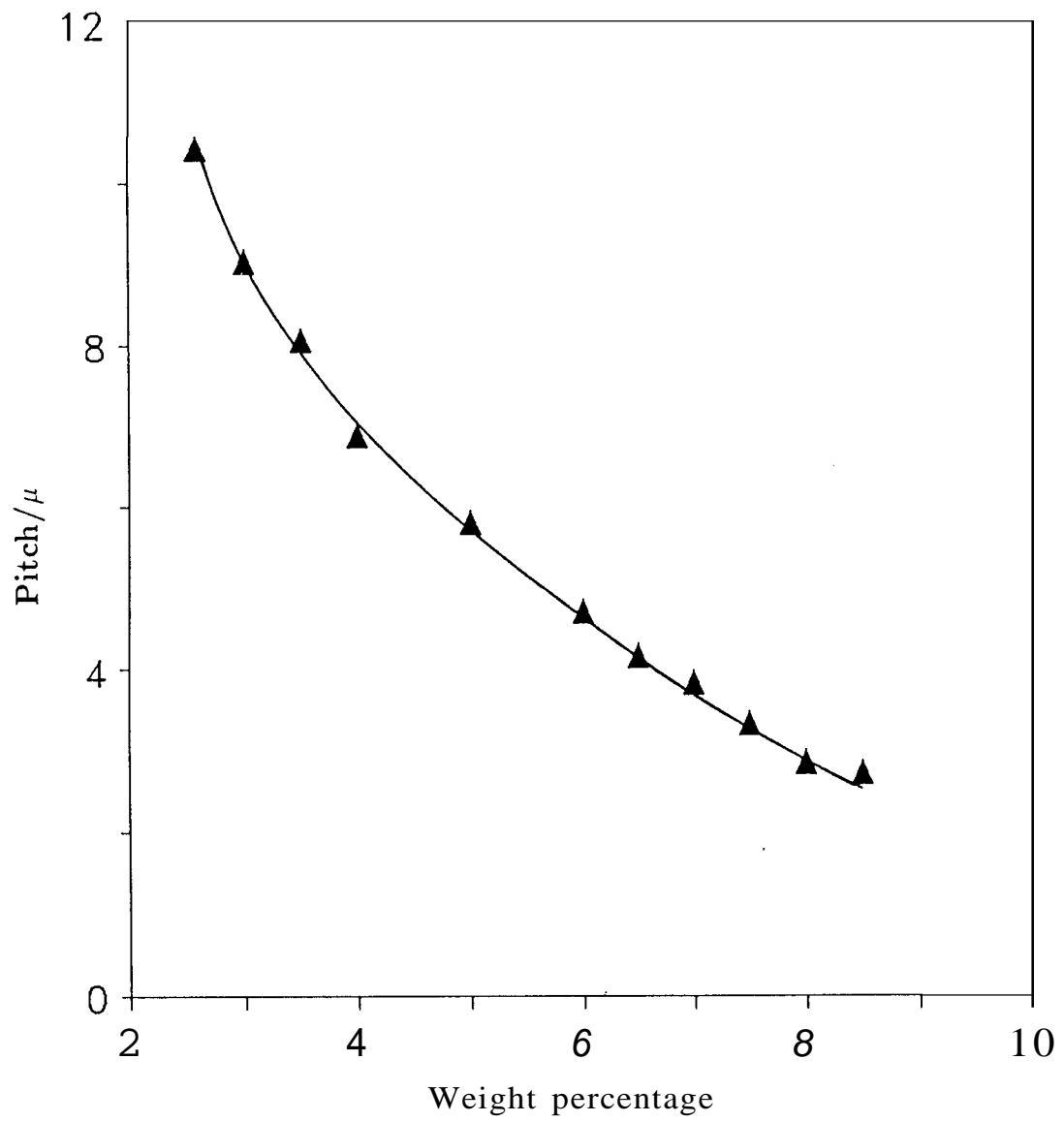


Figure 2.9. The plot of pitch versus the weight percentage of cholesteryl chloride in the nematic mixture. The continuous line has been drawn as a guide to the eye.

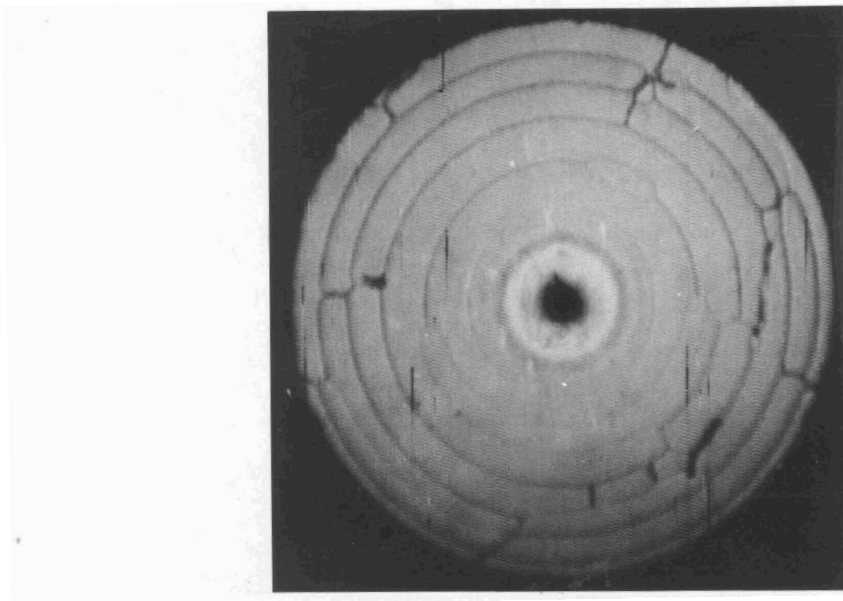


Figure 2.10. Photograph of the disclination rings used to find the handedness of the helix in the sample.

#### 2.4.4 Preparation of the cell

Indium tin oxide coated glass plates which were conducting and transparent were used to make the cells. Two glass plates were cut to the required shape and size. They were thoroughly cleaned. Two strips of spacers cut from a mylar sheet of suitable thickness, and smeared with an epoxy adhesive were sandwiched between the two plates in order to maintain a uniform thickness (Fig.2.11). The adhesive was cured by placing the cell in an oven maintained at a temperature of 150°C for 90 mins.

#### 2.4.5 Measurement of thickness of the air gap in the cell

We measured the thickness of the air film between the two glass plates of the cell using a channeled spectrum (Fig.2.12). Light from a source 'O' was rendered parallel by a lens  $L_1$  and was allowed to fall normally on the air film between the glass plates of the cell. The parallel reflected rays from the air film were made to converge on the slit of a constant deviation spectroscopy (Adam and Hilger Ltd.). An interference pattern was seen in the field of view of the spectroscopy. It consisted of alternate bright and dark fringes due to the interference of light reflected from the two surfaces bounding the air film.  $\lambda_m$  the wavelength corresponding to the  $m^{\text{th}}$  dark fringe and  $\lambda_{(m+n)}$ , the wavelength corresponding to the  $(m + n)^{\text{th}}$  dark fringe were directly measured from the spectroscopy. The thickness of the air film was calculated using the expression,

$$d = \frac{\lambda_{(m+n)} \lambda_m}{(\lambda_{(m+n)} - \lambda_m)} \times \frac{n}{2}$$

The cell was filled with the liquid crystal which was mixed with a few per cent of Lixon in the isotropic phase by capillary action. Observations were made under

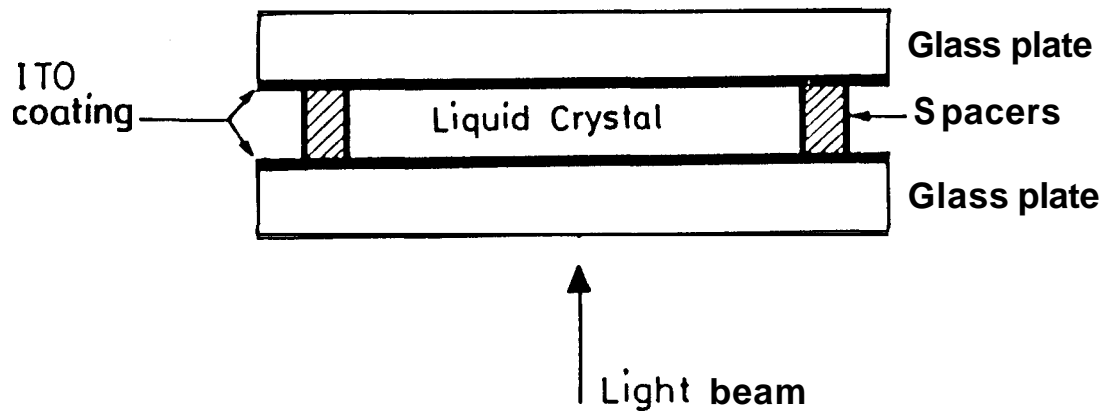


**Figure 2.11.** Geometrical configuration of the cell.

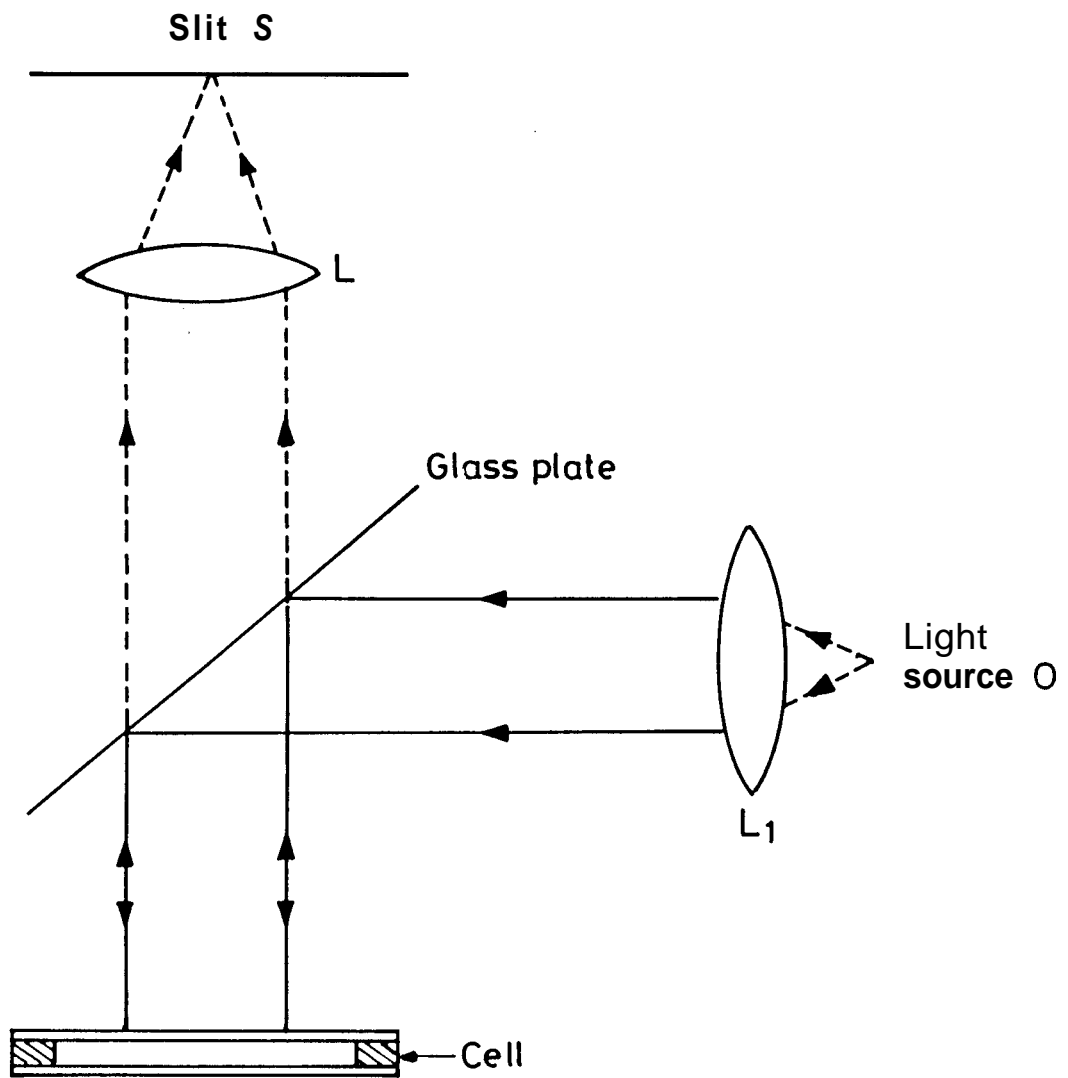


**Figure 2.12.** Arrangement to measure the thickness of the cell by forming the channelled spectrum.

a polarising microscope (Model Ortholux IIPOL-BK) on cholesteric drops having a flattened appearance as described earlier.

## 2.5 Results and Discussion

A DC electric field was applied between the electrodes, but no change was observed as the voltage was gradually increased from 0 to about 1.5 to 2 V, depending on the composition. At this voltage, the dark brushes became curved so that all of them had the same sense of curvature. A rearrangement in the director configuration is responsible for this curvature. Then the whole structure started rotating. The defect on the periphery of the drop was used as reference for measuring the angular velocity. The time taken for 10 rotations was measured and the average time taken for one rotation was calculated. This was repeated thrice for each drop. Then the applied voltage was increased in steps of 0.2 volt and the whole procedure was repeated for different applied voltages. Beyond about 3.6 volt, the structure itself got distorted and hence measurements could not be made. The electromechanical coefficient was calculated by the equation.

$$\frac{d\phi}{dt} = \frac{\nu_E E}{3\gamma_1} \quad (2.27)$$

For this purpose,  $d\phi/dt$  was plotted against the applied voltage. Using the slope of the linear part of this curve and assuming that the rotational viscosity coefficient  $\gamma_1 = 0.07 \text{Nsec/m}^2$ , a typical value for a room temperature nematic (see, for example, de Gennes, 1975) the value of  $\nu_E$  was calculated.

This experiment was repeated for different values of the pitch in the range 4-10  $\mu\text{m}$  which was obtained by varying the percentage of cholesteric chloride in the mixture. If  $P$  is  $\leq 4\mu\text{m}$ , for samples of  $D = 8\mu\text{m}$ , there would be two pitches at the lateral curved edge of the drops and in this case the structure of the drop itself

changes periodically under the action of the field. The central flat part winds up to a finger print configuration which spirals from the centre and then unwinds to give the planar texture once in a while. For large values of pitch ( $\geq 12\mu m$ ) the  $\chi$  defect in the drop moves to the centre and this configuration is not suitable for the experiment.

$d\phi/dt$  is shown as a function of the applied voltage  $V$  in one set of experiments on cholesterics with different values of pitch in figure 2.13. The thicknesses of all the samples were comparable, in the range of 8 to 10  $\mu m$ . It is seen that the slope increases as the pitch decreases. It is also noteworthy that the redox potential appears to gradually decrease from 2 to 1.5 V as the cholesteryl chloride content increases in the mixture.

To get a cholesteric with infinite pitch we added the two oppositely handed components, viz., 3 per cent by weight of cholesteryl chloride and 7 per cent by weight of methylbutylbenzyloxy heptyloxy cinnamate (see Fig.2.6) in the binary mixture of alkoxy phenyl-trans-alkylcyclohexyl carboxylates. The flattened drops formed by adding  $\sim 10$  per cent of Lixon had a bipolar configuration. We did not notice any perceptible rotation of the structure in the drops (Fig.2.14a and b) in spite of applying a sufficiently strong DC electric field across the sample and waiting for a long time, thus showing that  $\nu_E = 0$  in this case.

$\nu_E$  is plotted vs.  $q$  in figure 2.15. It is clearly seen from the figure that the coefficient  $\nu_E$  varies linearly with the wavevector  $q$ . The line passes through the origin, i.e.,  $\nu_E \propto q$  as predicted by the hydrodynamic theory. The value of  $\nu_E/q$  is found to be equal to  $-0.035 \text{ N/Vm}^2$ . This result shows that  $\nu_E$  is essentially of structural origin with no detectable contribution from the molecular chirality. However, we have to point out that the mixtures used in this experiment have only

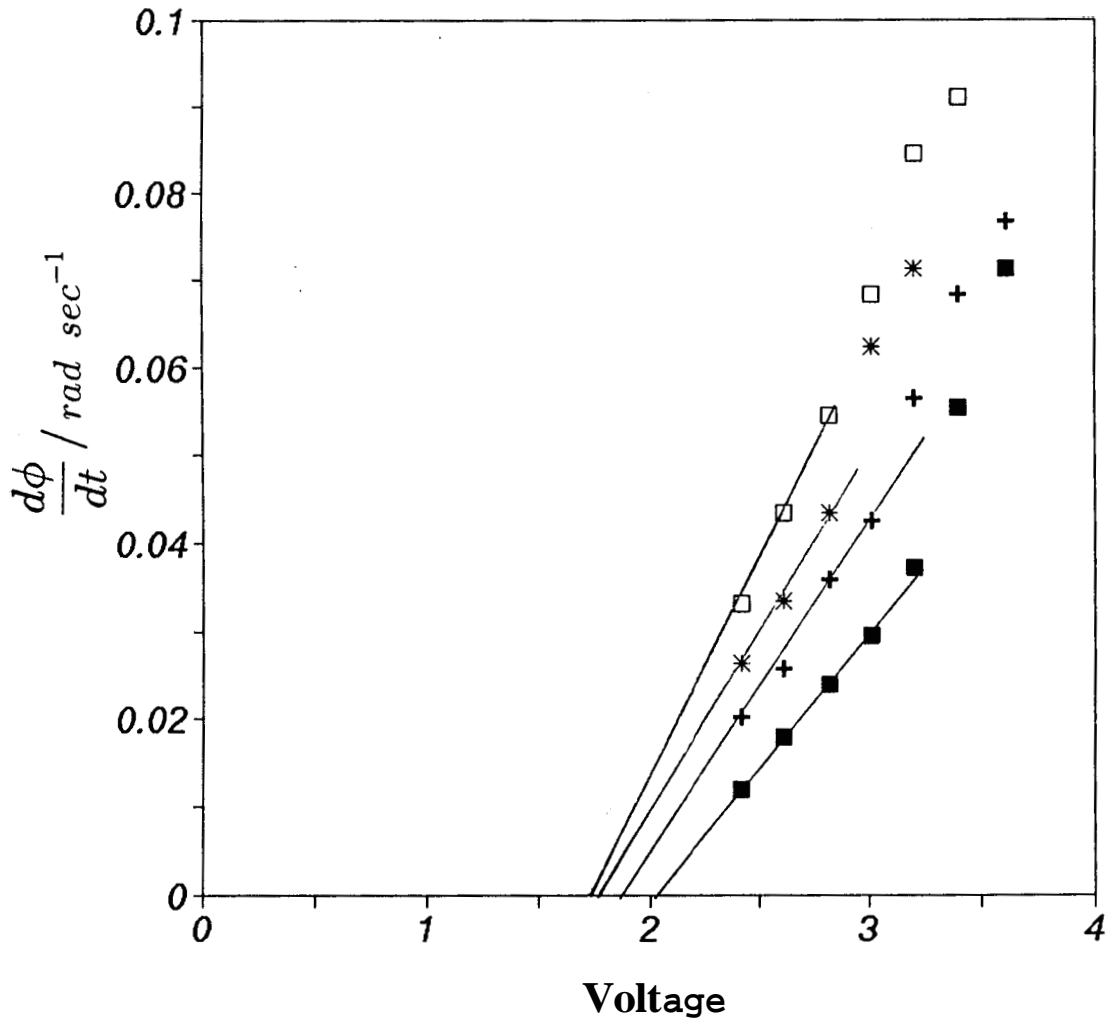
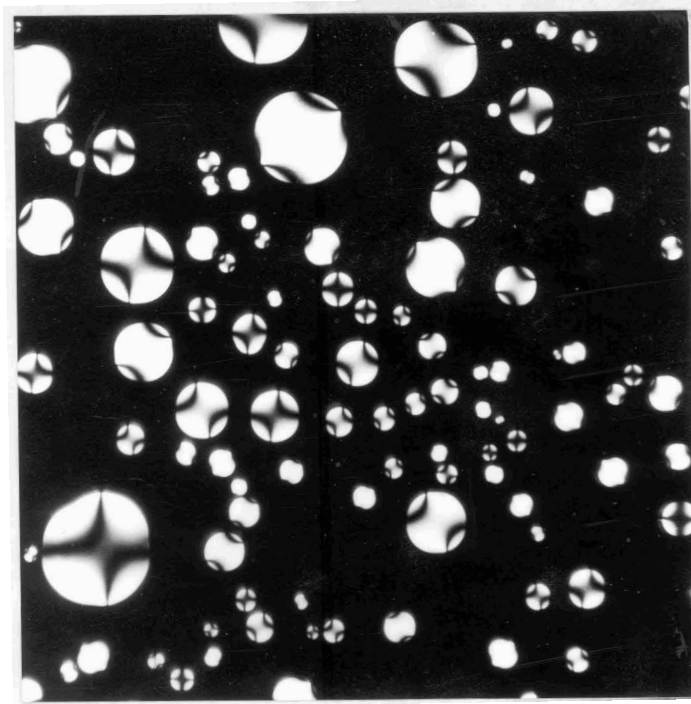


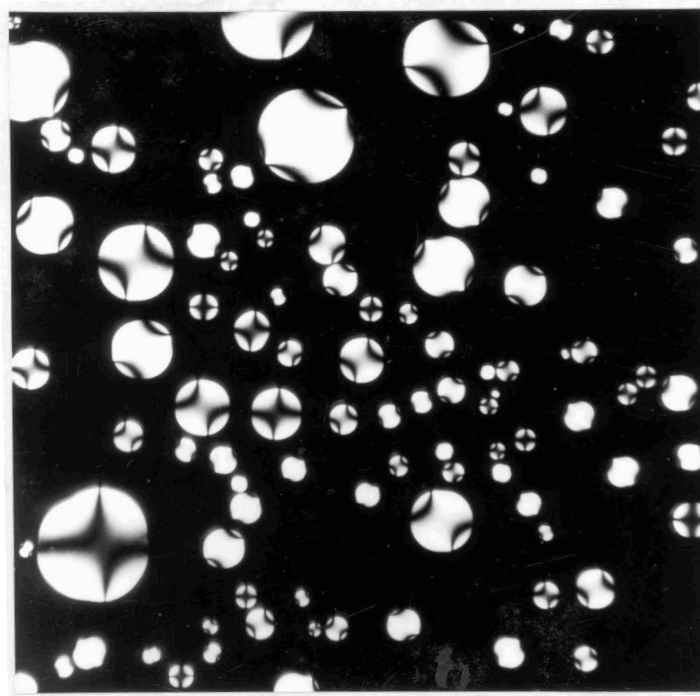
**Figure 2.13.** The plot of  $d\phi/dt$  as a function of applied voltage  $V$  for different values of pitch ( $P$ ) of the cholesteric sample.

- |   |                  |   |                  |
|---|------------------|---|------------------|
| □ | $P = 5.8 \mu m$  | * | $P = 6.8 \mu m$  |
| + | $P = 8.55 \mu m$ | ■ | $P = 10.4 \mu m$ |





(a)



(b)

**Figure 2.14.** Photographs of the compensated cholesteric drops. (a) 5 minutes after the application of 3 volt to the cell. (b) 20 minutes after the application of 3 volt to the cell.

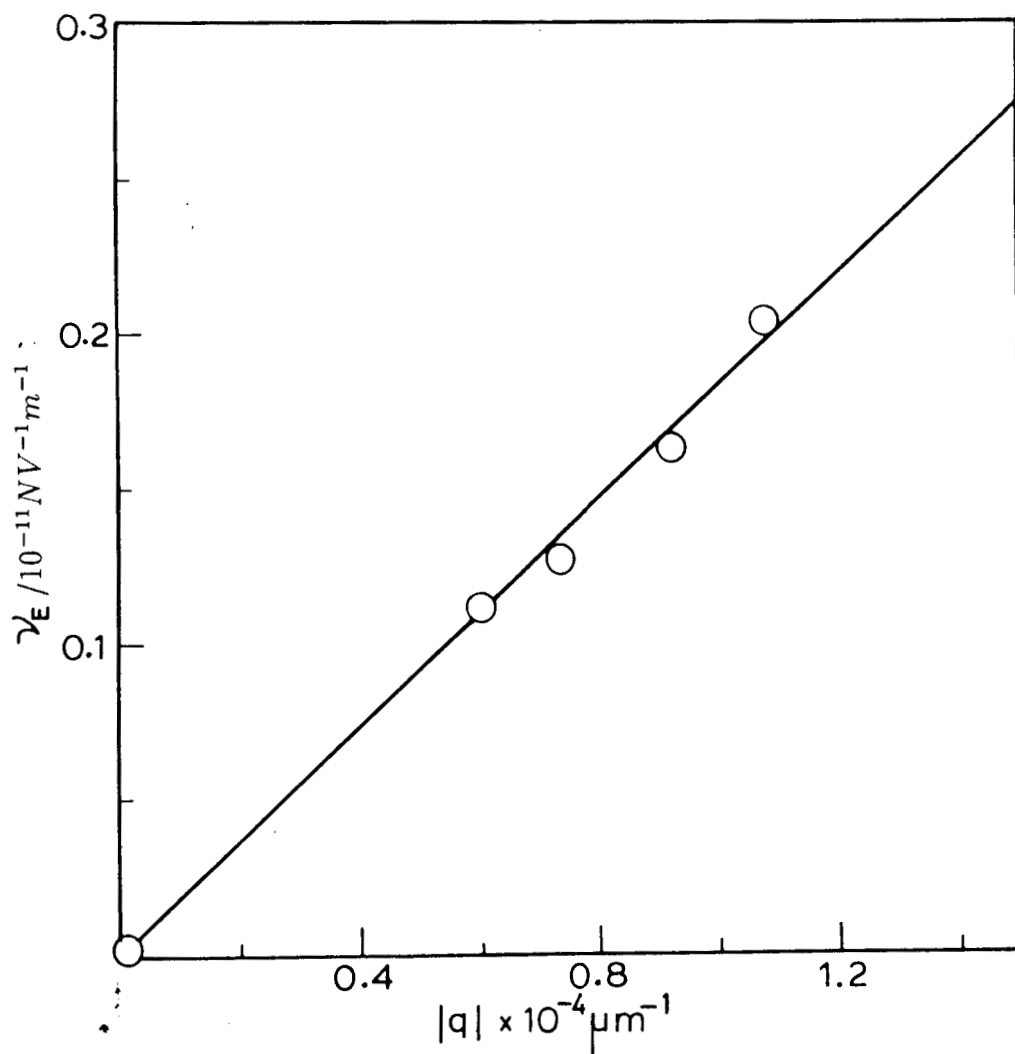


**Figure 2.15.** Plot of the electromechanical coupling coefficient  $\nu_E$  as a function of  $q$  ( $=2\pi/p$ ).

$\sim 10\%$  of chiral components. In fact, of all the compositions, the compensated mixture had the highest amount of chiral additives. This ensures that the basic chemical compositions of the mixtures are similar to a good approximation. This in turn gives rise to the linear variations of  $\nu_E$  vs.  $q$ .

As the chiral content in these mixtures is relatively small, it may seem that the molecular contribution to  $\nu_E$  may be masked by the structural contribution.

In chapter IV, we will present a different type of experiment in which the compensated mixture has  $\blacksquare$  60 per cent of the cholesteric material.

## References

BLINOV, L.M., 1983, *Electro-optical and Magneto-optical properties of Liquid Crystals* (John Wiley & Sons).

See for example, BOCCARA, N. (Editor), 1981, *Condensed Matter Physics, (IDSET)*.

CANO, R., and CHATELAIN, P., 1961, *C.R. Acad Sci*, 253, 2081.

CURIE, P., 1894, *J. Phys. Theor. Appl.*, 3, 393.

DE GENNES, P.G., 1975, *Tile Physics of Liquid Crystals* (Clarendon Press).

DE GENNES, P.G., 1976, in *Molecular Fluids*, Eds. R. Balian and G. Weill (Gordon & Breach, London), p.373.

EBER, N. and JANOSSY, I., 1982, *Mol. Cryst. Liquid Cryst.*, 72, 233.

EBER, N. and JANOSSY, I., 1984, *Mol. Cryst. Liquid Cryst.*, **102**, 311.

GRANDJEAN, F., 1921, *C.R. Acad. Sci.*, 172, 71.

IMURA, H. and OKANO, K., 1973, *Phys. Lett.*, **42a**, 403.

JAYARAM, H.K., KINI, U.D., RANGANATH, G.S., and CHANDRASEKHAR, S., 1983, *Mol. Cryst. Liquid Cryst.*, **99**, 155.

KASSUBEK, P., and MEIER, G., 1969, *Liquid Crystals*, Vol. 2, Ed. G.H. Brown (Gordon and Brech, New York), p.753.

- LESLIE,F.M., 1968, Proc. Roy. Soc., **A307**, 359.
- LESLIE,F.M., 1979, In Advances in Liquid Crystals, Vol. 4,  
Ed. G.H.Brown (Academic, New York),p.1.
- LEHMANN,O., 1900, Annln. Phys., 2, 649.
- LUBENSKY,T.C., 1972, Phys. Rev. A, 6, 452.
- LUBENSKY,T.C., 1973, Mol. Cryst. Liquid Cryst., 23, 99.
- MADHUSUDANA,N.V., and PRATIBHA,R., 1987, Mol. Cryst.  
Liquid Cryst. Lett., **5(2)**, 43.
- MADHUSUDANA,N.V., and PRATIBHA,R., 1989, Liquid Crystals, **5(6)**, 1827.
- MARTIN,P.C., PARODI,P., and PERSHAN,P.J., 1972, Phys. Rev. **A6**, 2401.
- OSEEN,C.W., 1933, Trans. Faraday Soc., 29, 883.
- PLEINER,H., and BRAND,H.P., 1987, Mol. Cryst. Liquid Cryst. Lett., 5, 61.
- PROST,J., 1972, Solid State Commun., 11, 183 and p.xiii.
- RANGANATH,G.S., 1983, Mol. Cryst. Liquid Cryst., 92, 105.
- ROBINSON,C., 1956, Trans. Faraday Soc., 52, 571.
- ROBINSON,C., WARD,J.C., and BEEVERS,K.R.B., 1958,  
Disc. Faraday Soc., 25, 41.